Laser-Cooled Continuous Cs-Beam Master Oscillator

H. Wang, W. F. Buell and G. Iyanu
Electronics and Photonics Laboratory
The Aerospace Corporation
Los Angeles, CA 90009
USA
he.wang@aero.org

Abstract— In this paper we present our design and prospects of a Magneto-Optical Trap (MOT)-based cold Cs-beam atomic clock physics package and report the realization and characterization of a continuous, laser-cooled Cs atomic beam from a Cs MOT. We have determined the longitudinal velocity of the cold Cs beam by Time of Flight (TOF) method to be 7 m/s with a velocity spread of 1 m/s. By adjusting the MOT parameters, we are able to tune the Cs-beam velocity from 5 m/s to 8.5 m/s while the velocity spread remains to be 1m/s. The Cs beam has an instantaneous atomic flux of 3.6×10^{10} atoms/s when operated in pulsed mode and a continuous beam flux of 2×10^{8} atoms/s. Our theoretical simulation reveals that the MOT inhomogeneous magnetic field and the varying Doppler shift along the atomic beam propagation play an important role in determining the longitudinal velocity of the Cs atomic beam. With the cold Cs beam thus formed and a compact Ramsey cavity of 13 cm in length, we have estimated a short-term, shot-noise limited Allan standard deviation of $2.7 \times 10^{-13}\ \tau^{-1/2}$ (τ is the averaging time) for the atomic master oscillator under development.

I. INTRODUCTION

There are continuing demands for better atomic master oscillators from global navigation and communication satellite programs. Laser-cooled low-velocity ($v < 10$ m/s) atomic beams have been considered feasible cold atom sources for developing compact and highly stable master oscillators for spacecrafts and satellite applications [1-4]. A cold atomic beam can be realized either by directly laser-decelerating a thermal atomic beam or by laser-accelerating an ensemble of ultra-cold ($T < 1$mK) atoms from a laser-cooled atom trap. The former usually requires a spatial distance of ~ 1 m to cool a beam of thermal atoms to the expected velocities, which defines the dimensions of the instrument [5-6]. However, the latter technique has the unique advantage of generating a useful cold atomic beam just outside the volume of a cold atom trap and hence could significantly reduce the size of the system.

The basic idea of the method is to introduce a controlled leak to a magneto-optical trap (MOT) by modifying the trapping potential in such a way that the MOT functions like a cold atom funnel, with which thermal atoms are captured, cooled and then pushed out to form an atomic beam [9-13]. Since the atomic beam thus formed originates from an ensemble of cold atoms at ~ 100 μK, very low beam velocities can be obtained within a short distance through a controlled laser acceleration process. In this paper we will first discuss our physics package of a cold continuous Cs-beam atomic clock using a 13 cm long Ramsey cavity. Then we will report our observation and investigation of a low-velocity Cs atomic beam generated from a vapor-cell Cs magneto-optical trap. In our system, no specially fabricated optics is used inside the vacuum chamber. We also separate the optical re-pumping laser beam from the laser beam responsible for accelerating the cold Cs atoms. In this way the Cs beam travels at an approximately uniform velocity after leaving the vicinity of the trap volume. A one-dimensional optical molasses is used to deflect the Cs beam away from the trapping laser beams. In Section III we will present our theoretical model that simulates the acceleration kinetics of the MOT-based Cs atomic beam. Finally we will discuss the prospects of the cold continuous Cs-beam atomic oscillator under development.

II. PHYSICS PACKAGE AND EXPERIMENTS

Fig. 1 schematically shows the physics package of the cold Cs-beam atomic clock. The slow-velocity Cs atomic beam, generated from a Cs MOT, is deflected by 30 degrees using a 1-D optical molasses [6-8]. The retro-reflected laser beam damps the velocity component perpendicular to the Cs-beam final propagation direction while leaves the velocity component along the final propagation path intact. The atomic beam deflection is necessary to prevent the Cs atoms from being perturbed by any MOT laser beams. Upon the Cs beam being deflected, optical pumping prepares Cs atoms into the magnetic-insensitive F=4, m_F=0 (or F=3, m_F=0) clock level before they enter a Ramsey microwave cavity of 13 cm in length. The optical pumping laser beam is also retro-reflected to prevent the Cs beam from being misaligned by the spontaneous force. Ramsey interference fringes and atomic clock signals will be generated via laser-induced fluorescence near the output of the microwave cavity. The 9.2 GHz microwave frequency from a tunable OCXO-based synthesizer will eventually be locked to the Cs atomic

0-7803-9052-0/05/$20.00 © 2005 IEEE.

hyperfine-transition to provide long-term frequency stability of the clock. The frequency stability of such a cold Cs-beam atomic clock will be discussed in Section IV.

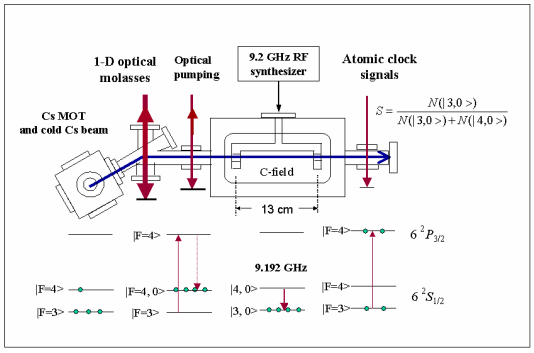

Figure 1. Schematic diagram of the clock physics package. The MOT laser beams are not shown here. The Cs atomic beam is deflected by 30 degrees using a 1-D optical molasses. Also plotted is the relevant Cs atomic energy levels as well as the optical pumping, clock interrogation and clock signal generation processes. The dimension of components is not in scale.

We generate the low-velocity Cs atomic beam from a vapor-cell MOT of Cs atoms. The MOT traps 8×10^7 Cs atoms with a density of 8×10^{10} atoms/cm^3 at ~ 300 μK. The Cs trap has a loading time constant of 0.4 s and is accommodated in an ultrahigh vacuum chamber with a background pressure of 6×10^{-10} Torr. A 150 mW Distributed-Bragg-Reflection (DBR) diode laser at 852 nm is used for cooling and trapping. The trapping laser frequency is 25 MHz red-detuned from the $6^2P_{3/2}$ F'= 5 hyperfine level. This red detuning is adjustable by tuning the RF frequency of an AOM driver.

The cold Cs beam is extracted from the Cs MOT by making one of the six trapping laser beams into a hollowed laser beam [13]. This configuration forms a controlled leak tunnel of the atomic trap while the MOT still captures and cools Cs atoms from the surrounding Cs vapor. The MOT optical re-pumping beam is introduced by co-propagating only with the vertical trapping beam, which is perpendicular to the Cs atomic beam. When the leak tunnel is established, the trapped Cs atoms feel a net spontaneous force from the acceleration laser beam, that is, the trapping laser beam propagating in the opposite direction of the hollowed trapping beam. A continuous Cs atomic beam is thus generated and imaged by laser-induced fluorescence in the vicinity of the trap volume as shown in Fig. 2. The bright spot in Fig. 2 is the Cs MOT cloud and the Cs beam is seen to the right of the trap.

We measured the mean velocity of the MOT-based Cs beam by the Time of Flight (TOF) method when the MOT-beam system is operated in a semi-continuous mode. A probe laser, focused to about 1 mm in diameter, crosses the atomic beam at a distance of 11 cm downstream from the MOT. As the Cs atoms pass through the probe beam, laser-induced fluorescence at the Cs D_2 line is recorded with a PMT. Fig. 3 shows a typical time of flight signal, where the horizontal axis is the flight time. Fig. 3 displays a TOF signal peaked at 15.1 ms, giving an averaged beam mean velocity of 7.3 m/s under typical experimental conditions. Note that the Cs atoms gain their full speed only in a short acceleration distance (less than 10% of the total flight path) and travel without further acceleration during most of their flight time. The line width (FWHM) of the TOF signal in Fig. 3 is 2.2 ms, corresponding to an atomic beam velocity spread of 1 m/s. This velocity spread is mainly due to the initial spatial and momentum distribution of the Cs atoms in the MOT volume (V ~ 1 mm^3 and T ~ 300 μK). Assuming all the 8×10^7 trapped Cs atoms pass through the probe laser beam in

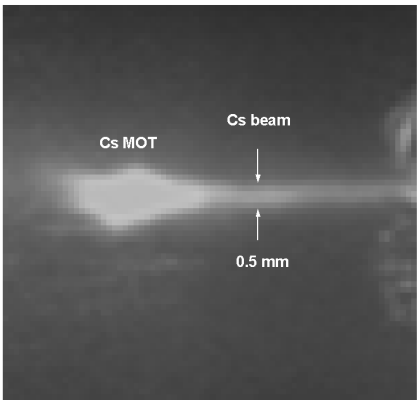

Figure 2. Laser-induced fluorescence image of the MOT-based continuous Cs atomic beam. The bright spot is the trapped cold Cs atom cloud and the relatively weaker narrow line is the Cs atomic beam traveling to the right.

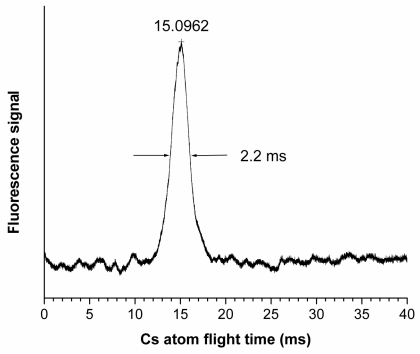

Figure 3. Time of flight measurement of the Cs atomic beam velocity. Laser-induced fluorescence is recorded at 11 cm downstream from the MOT center when the system is operated in a semi-continuous mode. The peak flight time gives a mean beam velocity of 7.3 m/s and the width (FWHM) of the signal indicates a velocity spread of 1 m/s.

2.2 ms, we have an instantaneous beam flux of 3.6×10^{10} atoms/s. If the cold Cs beam is operated in a continuous

mode and the Cs beam is the predominant trap loss, the continuous beam flux is approximately equal to the Cs MOT loading rate, which is measured as 2×10^8 atoms/s.

Our experiments also show that the Cs atomic beam velocity is tunable by adjusting the MOT parameters. Using the time of flight technique, we have been able to measure the velocity dependence on the acceleration laser frequency, the MOT magnetic field gradients and the acceleration laser intensity. The results are plotted in Fig. 4. In our experiment, the Cs atoms are accelerated by one of the trapping laser beams, whose frequency is red-detuned by a few times of the natural line width γ(5.18 MHz). Fig. 4a shows that a larger red detuning, δ_0/γ, reduces the velocity of the Cs beam. Here $\delta_0 = \nu_L - \nu_0$ is the red detuning of the acceleration laser and ν_L and ν_0 the laser frequency and the atomic resonance frequency, respectively. From Fig. 4b we have that the Cs-beam velocity decreases as the magnetic field gradient increases. This is because the Zeeman effects from the inhomogeneous magnetic field increase the total off-resonance detuning of the acceleration laser, resulting in a reduced spontaneous force as indicated in (3) and as designated in Fig. 6. The error bars in Fig. 4 are one standard deviation of the statistical uncertainty of the measured atomic beam mean velocity. The experiment shows that the Cs beam velocity can be tuned in a range of 5 – 8.5 m/s with a velocity spread of 1 m/s by adjusting the MOT parameters. The ability to control the atomic beam velocity is useful in implementing a highly stable atomic beam by actively stabilizing the beam velocity.

In Fig. 5 we demonstrate the spatial trajectory of the cold Cs atomic beam interacting with the 1-D optical molasses, which is designed to bend the atomic beam by an angle of 30^o. Our deflection laser beam has a cross-section of 15 mm in diameter and an intensity of approximately twice the Cs D_2-line saturated absorption intensity (I_s= 1.09 mW/cm^2). The cold Cs atomic beam extracted from the MOT has a nominal velocity of v=7.3 m/s and velocity components along x and z axis v_x=6.3 m/s and v_z=3.7 m/s, respectively. The x-axis is the Cs beam propagation path after being deflected. The v_z component, perpendicular to the x axis, is being damped by the 1-D molasses through the velocity-dependent force F [14]:

$$F = -\beta v \tag{1}$$

$$\beta = 4\hbar k^2 \frac{2S_0\delta/\gamma}{[1+4(\delta/\gamma)^2]^2}, \tag{2}$$

where k is the photon momentum and γ the natural linewidth of Cs D_2 transition. δ is the off-resonance detuning of the molasses laser and $S_0 = I/I_s$ stands for the saturation parameter with I and I_s the laser intensity and the saturation intensity, respectively. Under the experimental conditions, the optical molasses laser has to have an off-resonance red-detuning $|\delta/\gamma| < 3.0$ in order to completely deflect the Cs beam of 7.3 m/s by an angle of 30 degrees.

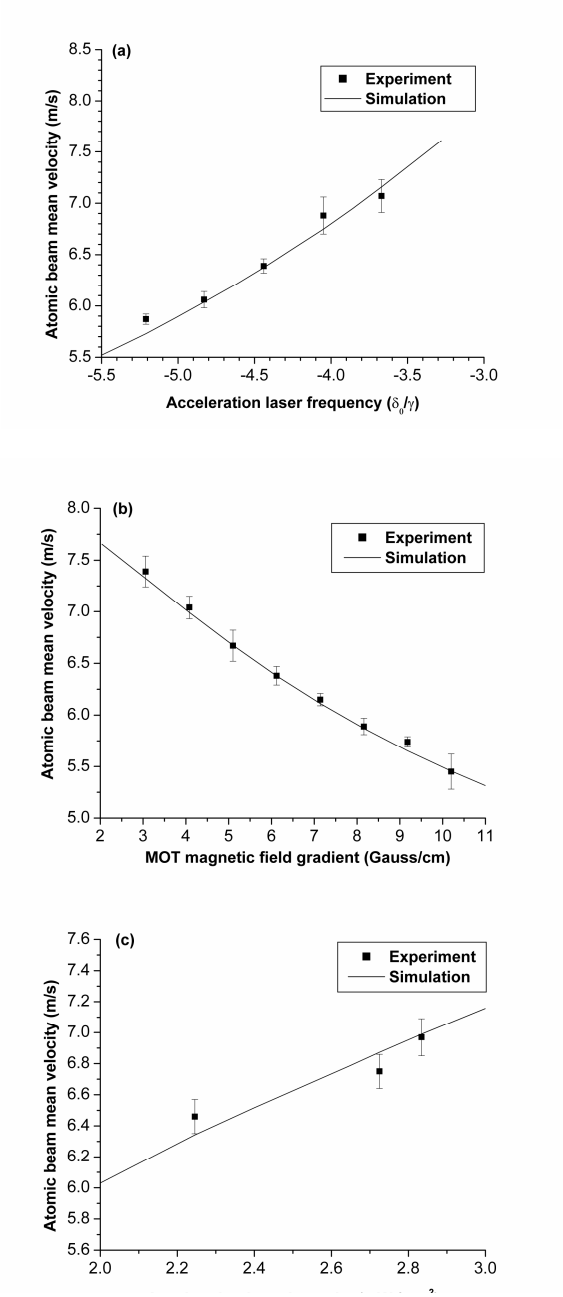

Figure 4. a) shows the measured and the calculated Cs-beam mean velocity as a function of the acceleration laser frequency red-detuned from resonance. b) compares the simulated Cs-beam mean velocity with the measured values as the MOT magnetic field gradient increases. The acceleration laser has a red detuning of $\delta_0 = -4.44\gamma$. c) shows the velocity dependence on the acceleration laser intensity.

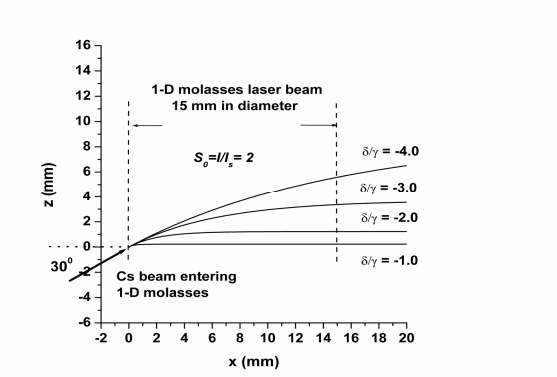

Figure 5. Spatial trajectory of the cold Cs atomic beam interacting with the 1-D optical molasses in the beam deflection region. Here x-axis is the atomic beam propagation path after deflection. δ is the red-detuning of the molasses laser and γ the natural linewidth of the atomic transition.

III. SIMULATION OF COLD CS BEAM VELOCITY

Since the Cs atomic beam is generated from a Cs MOT, the ultra-low trap temperature (300 μK) corresponds to a thermal velocity of ~ 20 cm/s for Cs atoms. Therefore we can ignore the initial thermal velocity of the cold atoms and consider only the longitudinal motion of the Cs atomic beam governed by the light-induced spontaneous force F_{sp} described in (3).

$$a = \frac{F_{sp}}{m_{Cs}} = \frac{\hbar k S_0 \gamma / 2 m_{Cs}}{1 + S_0 + (2\delta/\gamma)^2} \tag{3}$$

where a is the acceleration of Cs atoms (with mass m_{Cs}). In order to analyze the interaction of the Cs atoms with the acceleration laser, Fig. 6 schematically shows the region near the MOT volume where the Cs atoms gain its velocity.

The optical re-pumping laser beam in Fig. 6 propagates perpendicularly to the acceleration laser beam and has a beam diameter of 20 mm. The optical re-pumping beam keeps Cs atoms absorbing photons and being accelerated. As designated in Fig. 6 this acceleration region has an effective linear distance of 10 mm. Once the Cs atoms move out of this region they are instantly pumped by the acceleration laser into the lower $F'' = 3$ level, causing the acceleration process stops. The Cs beam then travels at an approximately uniform velocity towards the beam deflection region. Since the acceleration laser beam is circularly polarized (σ^+) it interacts only with Cs atoms in the $m_F = +1$ level. In the vicinity of the MOT volume, the Zeeman shift increases approximately linearly as Cs atoms move out of the MOT volume. In addition, as the Cs atoms gain their speed, the Doppler shift also adds to the effective off-resonance detuning (the Cs beam travels in the same direction as the acceleration laser beam does). We therefore have the total off-resonance detuning for (3):

$$\delta = \delta_0 + \mu B_x/\hbar + \Delta\nu_D \tag{4}$$

$$\delta_0 = \nu_L - \nu_0 \tag{5}$$

$$B_x = (\partial B/\partial x)x \tag{6}$$

$$\Delta\nu_D = (v/c)\nu_0, \tag{7}$$

where δ_0 is the fixed detuning of the acceleration laser and $\mu = \mu_0$ the Bohr magnetic constant for the relevant atomic transition. The magnetic field gradient $\partial B/\partial x$ is a parameter set by the MOT-coil current. $\Delta\nu_D$ stands for the Doppler shift at velocity v, and ν_0 = 351725718.50 MHz is the Cs D_2 line resonance frequency [15]. Substituting (4) - (7) into (3), we have

$$a = \frac{a_0 S_0}{1 + S_0 + [\frac{2}{\gamma}(\delta_0 + \frac{\mu}{\hbar}\frac{\partial B}{\partial x}x + \frac{\nu_0}{c}\mathrm{v})]^2}, \tag{8}$$

where $a_0 = \hbar k\gamma/2m_{Cs}$ is a constant determined by the Cs mass and the photon energy.

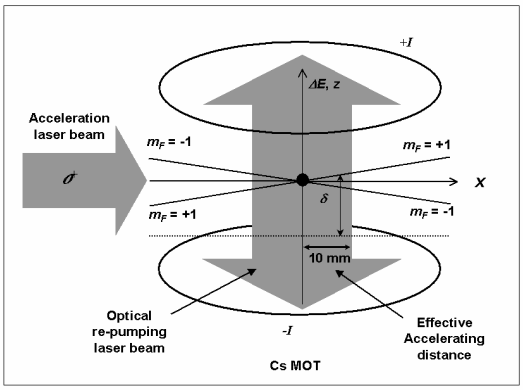

Figure 6. Schematic diagram of the acceleration region of the MOT-based Cs atomic beam. The x-axis is the direction in which the Cs beam travels. The solid, round dot at x = 0, z = 0 represents the trapped Cs atomic cloud. The MOT anti-Helmholtz coils generate an approximately constant magnetic field gradient ∂B/∂x in the vicinity of the MOT center. The two crossed lines, labeled with m_F = +1 and m_F = -1, represent the simplified atomic hyperfine levels under Zeeman effects. The vertical axis also stands for the relative energy ΔE to the atomic resonance, and the horizontal dashed line with ΔE < 0 indicates the red-detuned acceleration laser frequency. Both the acceleration laser beam and the optical repumping laser beam are circularly polarized. δ is the total off-resonance detuning of the acceleration laser.

In a similar way, the optical re-pumping laser also becomes off resonant by $\delta' = \mu B_x/\hbar$, $B_x = (\partial B/\partial x)x$, due to the Zeeman effects once the Cs atoms leave the MOT volume. However, Doppler effects can be ignored here, as the re-pumping laser beam is perpendicular to the Cs atomic beam. Therefore the optical re-pumping becomes less efficient as the Cs atoms travel in the x direction. This effect

is incorporated into the model by multiplying (8) with a Lorentzian function, and if writing $a = d^2x/dt^2$ and $v = dx/dt$, (8) becomes

$$\frac{d^2x}{dt^2} = \frac{a_0 S_0}{1 + S_0 + [\frac{2}{\gamma}(\delta_0 + \frac{\mu}{\hbar}\frac{\partial B}{\partial x}x + \frac{v_0}{c}\frac{dx}{dt})]^2} \times \frac{a' S_0'}{1 + S_0' + (\frac{2}{\gamma}\frac{\mu}{\hbar}\frac{\partial B}{\partial x}x)^2}$$

where $S_0' = I_{repump} / I_s$ is the saturation factor for the optical re-pumping laser beam and a' is a proportional constant.

The above nonlinear equation is solved numerically under the initial conditions $x = 0$ and $dx/dt = 0$ at $t = 0$. The results are plotted in Fig. 4 as solid lines and compared with the measured results. Fig. 7 gives the calculated Cs-beam velocity as a function of traveling distance x. The solid line simulates an acceleration process under typical experimental conditions. At $x = 10$ mm, where the acceleration ends, the Cs beam has gained a velocity of 7.4 m/s, which agrees with the measurement. The simulation indicates a much faster acceleration if Zeeman and Doppler effects are not considered as shown in Fig. 7 with dashed and dotted lines.

We attribute the good agreement between theory and experiment shown in Fig. 4 to the explicit inclusion of the varying Zeeman and Doppler effects in the simulation.

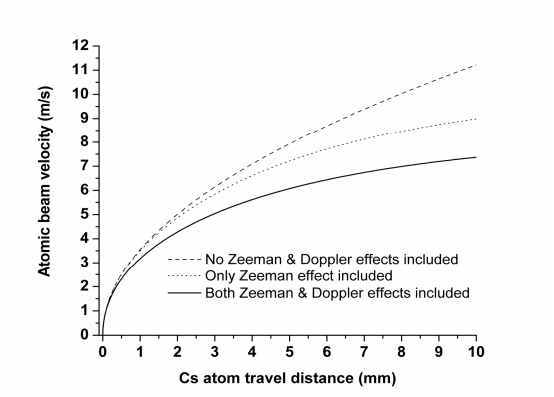

Figure 7. Calculated Cs-beam velocity as a function of the distance from the MOT in the effective acceleration region.

IV. CLOCK PROSPECTS AND CONCLUSIONS

Based on the measured cold Cs atomic beam parameters, we have estimated that the atomic master oscillator has an Allen standard deviation of $\sigma_y(\tau) = 2.7 \times 10^{-13}\ \tau^{1/2}$ (τ in second) for its short-time frequency stability under the shot-noise approximation [16-17]. Table I lists the estimated clock parameters. We also plot in Fig. 8 the Allan standard deviation $\sigma_y(\tau)$ as a function of the averaging time, giving an one day frequency stability of 9.2×10^{-16}.

In conclusion, we have designed the physics package of a continuous cold Cs beam atomic master oscillator and experimentally demonstrated a MOT-based cold Cs atomic beam, which travels at an uniform velocity of 7 m/s with a velocity spread of 1 m/s. The dependence of the cold atomic beam velocity on the MOT parameters has been experimentally and theoretically investigated. By adjusting the MOT parameters, we are able to tune the atomic beam velocity in a range of 5 – 8.5 m/s. We have developed a nonlinear mathematical model to simulate the spontaneous force responsible for the acceleration of the MOT-based Cs beam. Our calculation reveals that the inhomogeneous MOT magnetic field and the varying Doppler shift in the acceleration region have strong effects on the longitudinal velocity of the Cs atomic beam. This laser-cooled cold Cs beam is being used to develop a compact Cs-beam atomic clock for satellite applications.

TABLE I. ESTIMATED CLOCK PARAMETERS.

Beam flux (F)	2×10^8 atoms/s
Beam velocity (v)	7 m/s
S/N ratio (shot-noise limited)	1.4×10^4
Ramsey separated-field cavity length (L)	13 cm
Clock line width ($\Delta\nu$)	35 Hz [16]
Clock frequency (ν_0)	9.192 GHz
Clock short-term stability ($\sigma_y(\tau)$ τ in second)	$2.7 \times 10^{-13}\ \tau^{-1/2}$

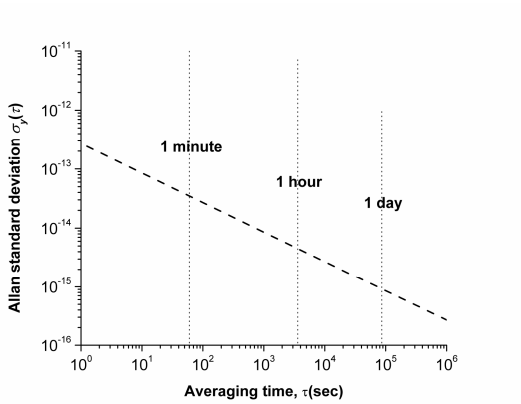

Figure 8. Estimated Allan standard deviation of the cold Cs-beam atomic clock using the measured Cs beam parameters.

ACKNOWLEDGMENT

The authors thank J. C. Camparo, Steven. M. Beck and B. Jaduszliwer for helpful discussions. This work was supported under The Aerospace Corporation's Mission Oriented Investigation and Experimentation program, funded by the U.S. Air Force Space and Missile Systems Center under Contract No. FA8802-04-C-0001.

REFERENCES

[1] Ph. Laurent, P. Lemonde, E. Simon, G. Santarelli, A. Clairon, N. Dimarcq, P. Petit, C. Audoin, C. Salomon, "A cold atom clock in the absence of gravity", Eur. Phys. J. D **3**, 201-204 (1998).

[2] T. P. Heavner, L. Hollberg, S. R. Jefferts, J. Kitching, W. M. Klipstein, D. M. Meekhof, H. G. Robinson, "Characterization of a cold cesium source for PARCS: Primary Atomic Reference Clock in Space", in Proceedings of 2000 IEEE International Frequency Control Symposium, pp. 656-658.

[3] C. Fertig, K. Gibble, W. M. Klipstein, L. Maleki, D. Seidel, R. Thompson, "RACE: Laser-Cooled Rb Microgravity Clock", in Proceedings of 2000 IEEE International Frequency Control Symposium, pp. 676-679.

[4] W. F. Buell, "Laser-pumped and laser-cooled atomic clocks for space applications", Laser and Particle Beams **16**, 627-639 (1998).

[5] H. S. Lee, S. E. Park, T. Y. Kwon, S. H. Yang,and H. Cho, "Toward a Cesium frequency standard based on a continuous slow atomic beam: preliminary results", IEEE Trans. Instr. Meas. **50**, 531-534 (2001).

[6] S. E. Park, H. S. Lee, E. J. Shin, T. Y. Kwon, and S. H. Yang, "Generation of a slow and continuous cesium atomic beam for an atomic clock", J. Opt. Soc. Am. B **19**, 2595-2602(2002).

[7] A. Witte, Th. Kisters, F. Riehle and J. Helmcke, "Laser cooling and deflection of a calcium atomic beam", J. Opt. Soc. Am. B **9**, 1030-1037(1992).

[8] A. Ashkin, "Atomic-beam deflection by resonance-radiation pressure", Phys. Rev. Lett. **25**, 1321-1324(1970).

[9] E. Riis, D. S. Weiss, K. A. Moler and S. Chu, "Atom funnel for the production of a slow, high-density atomic beam", Phys. Rev. Lett. **64**, 1658-1661 (1990).

[10] Z. T. Lu, K. L. Corwin, M. J. Renn, M. H. Anderson, E. A. Cornell and C. E. Wieman, "Low-velocity intense source of atoms from a magneto-optical trap", Phys. Rev. Lett. **77**, 3331-3334 (1996).

[11] K. H. Kim, K. I. Lee, H. R. Noh and W. Jhe, "Cold atomic beam produced by a conical mirror funnel", Phys. Rev. A **64**, 013402 (2001).

[12] A. Camposeo, A. Piombini, F. Cervelli, F. Tantussi, F. Fuso, E. Arimondo, "A cold Cesium atomic beam produced out of a pyramidal funnel", Optics Communications **200**, 231-239 (2001).

[13] H. Wang and W. F. Buell, "Velocity tunable magneto-optical-trap-based cold Cs atomic beam", J. Opt. Soc. Am. B **20**, 2025-2030(2003).

[14] Harold J. Metcalf and Peter van der Straten, Laser Cooling and Trapping (Springer-Verlag, New York, 1999).

[15] Th. Udem, J. Reichert, T. W. Hansch, and M. Kourogi, "Absolute optical frequency measurement of the Cesium D_2 line", Phys. Rev. A **62**, 031801(R)(2000).

[16] F. G. Major, The Quantum Beat, The Physical Principles of Atomic Clocks (Springer-Verlag, New York, 1998).

[17] J. Vanier and L. Bernier, "On the signal-to-noise ratio and short-term stability of passive Rubidium frequency standards", IEEE Trans. Instr. Meas. IM-**30**, 277-282 (1981).